



TITLE:

THE SAWAI LABORATORY

AUTHOR(S):

Sawai, Ikutaro

CITATION:

Sawai, Ikutaro. THE SAWAI LABORATORY. The Commemoration volume for the silver jubilee 1951: 28-35

ISSUE DATE:

1951-02-15

URL:

<http://hdl.handle.net/2433/74804>

RIGHT:

THE SAWAI LABORATORY

Head: Prof. Dr. Ikutaro Sawai

The papers published by this Laboratory cover the vast field of silicate chemistry including glass, enamel, refractory, porcelain, cement, roofing tile and ceramic furnace.

In the following they are tabulated according to their research items.

Glass

- 1) Softening of Glasses at High Temperatures (1937), J. Soc. Glass Tech., **21**, 113 (1937).
- 2) Influence of Gases on Properties of Glass at High Temperatures (1937-1939), Bull., **9**, 127 (1939); Z. anorg. u. allgem. Chem., **232**, 424 (1937).
- 3) Two Phase Glass (1937-1943), Bull., **8**, 118 (1938); **9**, 131 (1939); J. Chem. Ind., **40**, 172 (1937); **41**, 62 (1938); **42**, 822 (1939), **46**, 87 (1943).
- 4) Specific Gravity of Soda-Lime-Silica Glasses. (1937-1940), Bull., **8**, 114 (1938); J. Chem. Ind., Jap., **40**, 426 (1937); **41**, 663, 667, 846 (1938); **42**, 236, 699, 701, 703, 881 (1939); **43**, 84, 87, 89, 90, 92, 93, 578, 582, 724 (1940).
- 5) Properties of Low Alkali Glasses and Low Boric Oxide Glasses (1933-1943), Bull., **3**, 115, 122 (1933); **7**, 23 (1937); **8**, 123 (1938); J. Chem. Ind., Jap., **46**, 87 (1943).
- 6) Spinning of Glass Fibers (1940-1944), Bull., **11**, 107 (1940); **12**, 45 (1941); **13**, 65, 77, 82, 89 (1944); J. Chem. Ind., Jap., **43**, 778 (1940); **44**, 685, 866, 868, 871, 967, 969 (1941); **45**, 104, 105 (1942); J. Jap. Ceram. Assoc., **50**, 31, 163, (1942); **52**, 17 (1944); Kagaku, **11**, 302 (1941).
- 7) Chemical Resistance of Optical Glass (1943-1944), J. Jap. Ceram. Assoc., **51**, 407 (1943).
- 8) Electrochemical Properties of Glasses (1947-1949), Bull., **17**, 56 (1949).
- 9) Bubbles in Glass (1949-1950), Bull., **19**, 53 (1949); **21**, 62 (1950).
- 10) Determination of Density Change of Glass by the Sink-float Method (1949-1951), Bull., **19**, 52 (1949); **20**, 54 (1950); **24**, 71 (1950); **25**, 62 (1951).

Porcelain Enamel

- 1) Mechanism of Adherence of Enamels to Steel Surface (1946-1950), Bull., **15**, 11 (1946); **16**, 34 (1947); J. Jap. Ceram. Assoc., **57**, 70, 86, 124, 149 (1949); **58**, 51, 204, 389 (1950).
- 2) Effects of Boric Oxide, Alumina and Titan on Properties of Ground Coat Enamel. (1949-1950), Bull., **17**, 49, 51 (1949); J. Jap. Ceram. Assoc., **57**, 30, 167 (1949); **58**, 133 (1950).
- 3) Titanium Enamel (1948-1950), Enamel Ind., Jap., **1**, (1), 7 (1948); **1**, (4), 11 (1948); **3**, (2), 6 (1950).
- 4) Molybdenum Enamel (1949-1950), Bull., **19**, 37 (1949); Enamel Ind., Jap., **2**, (3), 9 (1949); J. Jap. Ceram. Assoc. **58**, 135 (1950).
- 5) Defects of Porcelain Enamel (1950-1951), Bull., **21**, 62 (1950); **23**, 60 (1950); **25**, 61 (1951); Enamel Ind. Jap., **3**, (1), 10 (1950); **3**, (6), 6 (1950); **4**, (2-3), 1 (1951); Memories of the Faculty of Eng. Kyoto Univ., **13**, 11 (1951); Finish, U. S. A. April, 33 (1951).
- 6) Electrostatic Spraying of Porcelain Enamel (1950-1951), Bull., **25**, 60 (1951).

Refractory

- 1) Sintered Corundum (1941-1946), Bull., **13**, 59 (1944); **15**, 13, 14, 15 (1946); J. Jap. Ceram. Assoc., **49**, 77 (1941); **50**, 143, 171, 172, 173 (1942).
- 2) Properties of Titanium Oxide (1949), Bull., **17**, 55 (1949).

Porcelain and Pottery

- 1) Takehara Potter Stone (1949), Bull., **17**, 53 (1949).
- 2) Glaze of Ceramic Ware (1949), Bull., **18**, 74, 76 (1949).

Cement

- 1) Cement Slate (1940), J. Chem. Ind., Jap., **43**, 937 (1940).
- 2) Activation of Blast Furnace Slag (1942), Bull. of Inst. Sci. Research, Manchuko, **6**, 432 (1942).
- 3) Automatic Shaft Kiln for Production of Portland Cement (1949), Bull., **18**, 1 (1949).

Roofing Tile

- 1) Roofing Tile (1949-1950), Bull., **18**, 78, 80 (1949); **19**, 34 (1949); **21**, 63 (1950); J. Jap. Ceram. Assoc., **57**, 20, 43 (1949).

Combustion and Industrial Furnaces

- 1) Gas Fired Furnace (1942-1949), Bull., **14**, 74 (1947); J. Jap. Ceram. Assoc., **51**, 8, 531 (1943); J. Chem. Ind., Jap., **46**, 75 (1943); Chem. Eng. Year Book, **7**, 160 (1949).
- 2) Combustion of Solid Fuels (1949-1951), J. Chem. Soc., Jap., Ind. Chem. Sec., **54**, 301 (1951).
- 3) Flow of Gases in Furnaces (1949-1951), Bull., **19**, 34 (1949).
(Bull. : Bull. Inst. Chem. Res., Kyoto Univ.)

Out of the above-mentioned problems studied under the direction of Prof. Sawai, some of the main results will be summarized below.

Determination of the Density Change of Glass

By M. Mine

The flotation method of measuring small variations in the density of glass was used successfully for the control of glass composition in tank-melting operations. Fundamental studies of this method were made to apply it to glass manufacturing in Japan. The density characteristics of glass melted in the pot-furnace of a factory were investigated by this method. The results indicates that the method is, in some occasions, available effectively even to small factories in this country.

It is well known that the density of glass is not only affected sensitively by variations in chemical composition, but depends considerably on thermal history. To get exact knowledge on the general features of the compacting process of glass, the density change of glass of a definite composition subjected to heat treatments was determined. The method was found to be very useful to a successive density determination of several samples, the density of which differs slightly each other.

1. Measurement of Density

The method of measuring glass density used was similar in principle to that of M. A. Knight (J. Amer. Ceram. Soc. **28**, 297 (1945)). But in 1948, when the the research was started, appropriate organic heavy liquids and special solvents such as used by Knight (l.c.), R. D. Duff (ibid., **30**, 12 (1947)) and A. T. Coe (J. Soc. Glass Tech., Trans. **33**, 199 (1949)) could not be obtained at all in this

country. Therefore, the water solution of K_2HgI_4 (Thoulet's solution, maximum density, ca. 3.2 g./cm.³) was used as buoyant liquid. (The complex salt was prepared in the laboratory with potassium iodide and corrosive sublimate.) As bromoform has become obtainable after 1950, mixtures of it with monobromobenzene, monochlorobenzene or dibutylphthalate were used. The characteristics of these organic mixtures as buoyant liquid were compared and checked with those of Thoulet's solution. In the range of density of 2.4-2.6 g./cm.³, the temperature coefficients of density of Thoulet's solution and the mixtures of organic liquids were found to be $11-12 \times 10^{-4}$ and $20-22 \times 10^{-4}$ (g./cm.³/°C), respectively. There was no noticeable difference between these liquids in accuracy of density measurement.

2. Density Characteristics of Glass Melted in the Pot-Furnace

The density characteristics of soda-lime glass of a relatively higher grade melted in the closed pot were investigated with the above-mentioned method. Measurements were made on a) changes in glass density with the lapse of time from the beginning of the fining period to the end of the working, b) difference in density due to difference in position from which the glass samples were taken out (the glass surface, center, bottom and wall-side in the pot), and c) changes in glass density due to pot corrosion.

The densities of glass samples taken out of the pot and annealed with a definite schedule were found to be nearly the same within the error of measurement (ca. 0.0002 g./cm.³), regardless of sampling periods from the reaching maximum melting temperature over 1400°C to the end of the working, or of the sampling position within the pot. But variations in glass density over 0.01 g./cm.³ were found to be almost unavoidable for each separate glass batch, because of roughness of the operation of manual weighing and batch handling for each charge.

Daily variations in glass density were also observed over 2 months' period. From these results, it seems that the method of measuring density is effectively applicable for quality control, in some occasions, even to small plants, which are operated with pot-furnaces.

3. Density Characteristics of Rod Samples

The density of glass rod drawn and cooled in air decreases with the decreasing diameter, and the difference in density caused by that in diameter disappears by annealing. The difference in density between the rod-as-drawn of a definite diameter and the sample annealed by a definite schedule is constant for glass of the same type, as shown in Fig. 1. The figures also indicate that the difference between densities of annealed- and rapidly cooled rod-samples increases nearly linearly with the decreasing diameter, as long as the latter lies in a narrow range, as disclosed by Duff (l.c.) with a certain flint and an amber glass. More exactly, however, the gradients of the curves representing the diameter-density relations increase more and more rapidly with the decreasing diameter. These differences in density between the annealed- and unannealed rod- samples can be explained, at least qualitatively, by the differences between the coefficients of thermal expansion above and below the transformation point, which are tabulated in Table 1.

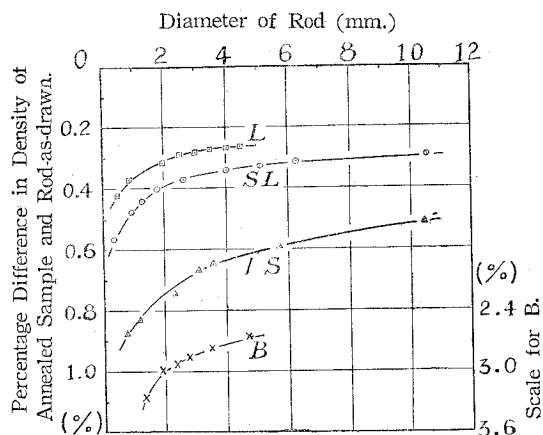


Fig. 1. The Relation between the Diameter and the Density of Rod-as-drawn.

- (L) Lead-(stem-) glass, the density of the annealed sample which was cooled down at the constant rate of $0.5^{\circ}\text{C}/\text{min.}$ from 480°C. $D_a=3.0804$ (g./cm^3).
 (SL) Soda-lime glass, $D_a=2.4984$ (from 600°C.)
 (B) B_2O_3 -glass, $D_a=1.8564$ (from 290°C.)
 (BS) Borosilicate optical glass, the density of fine annealed sample, $D_a=2.5167$.

Table 1. Thermal Expansion Characteristics of Glasses

Type of Glass	Deformation Point D. P. ($^{\circ}\text{C}$)	Transformation Point T. P. ($^{\circ}\text{C}$)	Cubical Coefficient of Thermal Expansion	
			Below T. P.	Above T. P.
1. Soda-Lime Glass	610	530	$2.7 \times 10^{-5}/^{\circ}\text{C}$	$12.8 \times 10^{-5}/^{\circ}\text{C}$
2. Borosilicate Glass	618	550	2.6 „	15.3 „
3. Lead Glass	498	440	2.8 „	9.0 „
4. Boric oxide Glass	298	250	5.0 „	45.5 „

4. Range of the Density Change Affected by Thermal History

The density of oil- and water-quenched samples of soda-lime glass was found to be smaller than that of rod-as-drawn, 4–5 mm. in thickness, by 0.2–0.3% ($55-70 \times 10^{-4} \text{ g./cm}^3$) and by 0.6–0.8% ($150-200 \times 10^{-4} \text{ g./cm}^3$), respectively. The density of such intensely quenched samples was increased by reheating at the temperature far below its annealing range. A water-quenched sample, for an example, proved the increase in density at the 3rd decimal place by heating for an hour at the temperature as low as 100°C.

The density of rod-as-drawn, 3–6 mm. in thickness, increases by 0.55–0.60% ($135-150 \times 10^{-4} \text{ g./cm}^3$), when treated at 450°C for about a month. Thus, the density of soda-lime glass of a definite composition varies readily at least in the range of over 1% ($0.02-0.03 \text{ g./cm}^3$) by difference in thermal history. Therefore, the change in density at the 4th decimal place, which is the degree of accuracy of the above-mentioned measuring method, can not be discussed without knowing the precise thermal history of the samples.

5. Density Change of Glass Subjected to Heat Treatments at Temperatures in the Annealing Range

For the purpose of obtaining exact knowledge on the change in glass density affected by different thermal history, the density of a soda-lime glass of a definite composition was measured after being subjected to different heat treatments. The results obtained are summarized as follows:

1) The density of rapidly cooled samples, after having been reheated for a definite time at different temperatures and cooled in air, was found to show a maximum value, when heated at a certain definite temperature. The maximum value in density, D_m (g./cm.³) and the temperature T_m (°C), at which this maximum value occurs, vary with the holding time t (minute) according to the equations: $D_m = D_{m.1} + d \cdot \text{Log}_{10} t \dots\dots(1)$ and $T_m = T_{m.1} - c \cdot \text{Log}_{10} t \dots\dots(2)$, where $D_{m.1}$ is constant for glass of a definite composition, but varies with small variations in the chemical composition of the sample. The temperature $T_{m.1}$ and the coefficients d and c are characteristic constants which are common to glass of this type, their values being 527°C, 0.0025 g./cm.³ (mean) and 18°C (mean), respectively. The efficient compacting temperature of glass for a definite time of holding may be found by the equation (2).

2) For each value in density D (g./cm.³) of glass, the rate of increase of D reaches the maximum at a certain temperature T_v . The temperature T_v (°C) at which the condition, $d(dD/dt)/dT=0$, is satisfied, was found to decrease with time t (minute) according to the equation: $T_v = T_{v.1} - c \cdot \text{Log}_{10} t \dots\dots(3)$, where $T_{v.1}$ and c are constant for glass of this type, having the values of 521°C and 18°C, respectively. Hence it may be said that the most efficient method of compacting glass is to lower temperature with the schedule represented by the equation (3).

3) It was also found that the density D_r (g./cm.³) of the glass sample which has been cooled from 600° to 350°C at a constant rate r (°C/min.) ranging 0.007-30°C/min., is expressed by the equation, $D_r = D_{r.1} - d \cdot \text{Log}_{10} r \dots\dots(4)$, where a constant density value $D_{r.1}$ corresponding to the cooling rate of $r=1^\circ\text{C}/\text{min.}$ varies with small variations in the chemical composition of the sample, but the coefficient d 0.0025 (g./cm.³) is constant for glass of this type and coincides with d in the equation (1) within the error of measurement. The result seems important for the purpose of comparing the density variations due to small variations in glass composition and of explaining the nature of the transformation point of glass.

Studies on the Mechanism of Adherence of Porcelain Enamels to Steel Surface

By M. Tashiro

The study of the mechanism of adherence of enamels to steel is essential with regard to the improvement of the mechanical strength of enameled steel wares. Hitherto, however, the microstructure of the enamel-steel interface has been investigated in most cases only by the microscopic observation of the cross-section of the enameled steel. Therefore, the structure of the portion especially near the interface, that is, within a few micron of it, has remained almost indistinct, because of the technical difficulties of observation.

With a view to obtaining a more clear picture of the structure of the enamel-steel interface, the author planned firstly to investigate the physico-chemical changes, which occur near the enamel-steel interface in practical firing process, and then, to summarize from the results the interfacial structure of normal fired enameled steel.

1. Consumption of Oxygen by Steel Surface during the Firing of Enamel

It is well known that oxygen in the air is necessary for the firing of enamel. Oxygen diffuses through the enamel layer and reacts with the steel surface. The author measured successively the volume of oxygen consumed by steel surface during the firing. The steel pieces applied with a ground coat by dipping were dried and put into a silica tube filled with oxygen at a pressure of 152 ± 5 mm. Hg. and heated to 885°C .

The composition of the frits used were as follows;

	SiO ₂	Al ₂ O ₃	CaO	Na ₂ O	K ₂ O	Co ₃ O ₄	B ₂ O ₃
(No. 1)	54.61	5.36	5.06	15.13	5.02	—	14.82 (difference)
(No. 2)	53.82	5.25	5.14	15.25	4.57	0.47	15.51 (difference)

The slip was prepared by adding clay 5 and ammonium carbonate 0.5 to 100 of the frit. The results indicates that the progress of the consumption of oxygen was divided into three stages; that is, 1) the oxidation of iron surface by oxygen, which passes freely through the unmelted frit particles, 2) the interval when oxygen consumption is stopped, and 3) the oxidation of iron surface by oxygen which diffuses through the melted frit. The velocity of the consumption of oxygen was the same for both specimens applied with enamel frits of No. 1 and No. 2; this means that the velocity of the diffusion of oxygen is not affected by the presence of cobalt oxide in the frit.

2. The Role of Ferrous Oxide during Firing

To make clear the cause of stoppage of oxygen consumption in the middle of firing, oxygen consumption was also measured with steel pieces, the surface of which was covered with a artificial ferrous oxide layer of 4—15 micron thick. The results indicates that the diffusion of oxygen through the molten enamel layer did not occur as far as the ferrous oxide layer exists between the enamel and the steel surface, and the diffusion began after the ferrous oxide layer disappeared by dissolving into the molten enamel layer. From this fact the following conclusion was made for the progress of the actual firing; 1) the stoppage of oxygen consumption is due to the existence of the primary ferrous oxide layer under the molten enamel layer formed during the first stage of the firing process, 2) after this ferrous oxide layer dissolves into molten enamel, no formation of a new ferrous oxide layer occurs between the steel and the enamel, 3) after the primary ferrous oxide layer disappears, the velocity of oxygen consumption is determined by the dissolution velocity of the ferrous oxide layer into the molten enamel layer.

3. The Dissolution Velocity of the Ferrous Oxide in Molten Enamel

The dissolution velocity of ferrous oxide into the molten enamel was determined. A layer of ferrous oxide, 0.5 mm. thick, was formed on a steel piece; this piece was dipped into molten frit No. 1 at $885 \pm 10^\circ\text{C}$ and, from the decrease of the thickness of the ferrous oxide layer, the diffusion constant (D) of the ferrous oxide in the molten frit was obtained. The value of (D) was found to be 0.66×10^{-7} cm./sec. The measurement was also made with frit No. 2, and it was found that the dissolution velocity was not affected by the presence of the small amount of

cobalt oxide. Using the above diffusion constant, the quantity of the ferrous oxide dissolved during the firing was calculated; it agreed well with the quantity of formed ferrous oxide determined from the oxygen consumption described in section 1.

4. Effects of the Temperature and the Chemical Composition of the Enamel Frit on the Dissolution Velocity of Ferrous Oxide

Enamel frit containing borax is believed to have a greater ability to dissolve ferrous oxide than borax free enamel. In order to ascertain if this is true, the dissolution velocities of ferrous oxide in enamel No. 1 and in the borax free sodium silicate, which has the same viscosity, were determined. It was found that the velocities were the same for both enamels. This seems to indicate that the diffusion velocity is not affected by the chemical composition of enamel, if the viscosities of enamels are same. The temperature and viscosity of enamel were found to affect velocity strongly. Their relation can be expressed in the following equation;

$$S(dl/dt) = \text{const. } l^{-Q/RT},$$

where Q : 53 kg.-cal./mol. (diffusion activation energy of ferrous oxide), S : density of ferrous oxide, and (dl/dt) : diminishing velocity of the thickness of ferrous oxide layer, and

$$S(dl/dt) = \text{const. } \eta^{-1.2},$$

where η : viscosity of enamel.

5. The Viscosity Gradient and Distribution of Ferrous Oxide in the Molten Enamel Layer during the Firing

The various amount of ferrous oxide was added to enamel frit No. 1 and the relation between the ferrous oxide content (C) and the viscosity (η) of the enamel were measured. The relation at 900°C was expressed in the following formula; $\log \eta = 0.030C + 3.5$.

By using this equation and the equation of diffusion of ferrous oxide in molten enamel, the distribution of ferrous oxide in the molten enamel layer during the firing was determined. The viscosity of enamel during the firing is lower at the steel surface than at the surface exposed to the air. It was concluded that wetting of the steel surface by enamel is greatly promoted by this decrease of viscosity at the steel surface.

6. Iron-Silicate Crystals Appearing at the Iron-Enamel Interface

At high temperature, enamel dissolves a considerable amount of ferrous oxide. Then, it is naturally expected that some crystals are separated out from enamel, when the enameled steel is withdrawn from the furnace. Kautz found, under the reflected light, gray crystals formed at the steel-enamel interface of the over fired enameled steel, and assumed them to be ferrous oxide. To clarify the nature of the gray crystals, the author prepared large crystals, which could be easily decided by petrographic examination. A steel ring having an artificial ferrous oxide layer, about 0.15 mm. thick, on the inner part of the ring was filled with enamel. Disk, 0.1 mm thick, was cut from the ring, and polished. Clear photomicrographs of the

iron-enamel interface at the inside wall of the ring showed the crystals about 100 times as large as those found in marketed enameled steel wares. These crystals were gray in the reflected light, but yellowish brown and transparent in the transmitted light. Contrary to other theories hitherto proposed they are naturally not ferrous oxide, but seem to be iron silicate. The optical properties of this yellowish-brown iron silicate were as follows; n about 1.75 or above, strong birefringence, +elongation, zero extinction angle, and no pleochroism. For the formation of crystals, SiO_2 , Na_2O , B_2O_3 and FeO are necessary, but Al_2O_3 , CaO and K_2O are not required. Some of the crystals contained crystals of fayalite and ferrous oxide in themselves especially near the steel surface. In this case, the structure of crystals were found to be very brittle and the enamel layer was liable to chip off from the base steel.

7. Distribution of Metallic Particles in the Enamel Phase

When a cross-section of enameled steel is examined in the reflected light, a string of metallic particles can be seen in the enamel phase of short distance from the iron base. These particles do not appear, when cobalt free enamel is used, and the appearance of these particles is only one characteristic feature of the enamel, when cobalt oxide is used to increase its adherence. Hitherto, no explanation has been given why these metallic particles take such a peculiar distribution. By a special method described in section (6), the author obtained a specimen in which large metallic particles appeared; the distribution of the particles was exactly same, but the size was more than about 100 times and, moreover, the distance between the particles and the steel surface was 10 -- 100 times of those observed in marketed enameled steel wares. By a microscopic study of the thin section of a specimen, using the transmitted light, it was found that (1) a string of metallic particles observed in the reflected light is the cross-section of a network which consisted of entangled minute needlelike metallic crystals and (2) the crystallization of the minute metallic crystals took place at the top of the diffusion of ferrous oxide in the molten enamel phase. The needle like metallic crystals thus formed were then pushed up by the gas bubbles evolved from the steel base and gathered to form the network.